Endogenous Separations and Non-monotone Beveridge Curve Shifts[†]

Hanbaek Lee *University of Cambridge*
Philip Schnattinger *Bank of England*
Francesco Zanetti *University of Oxford*

February 14, 2026
(click here for the latest version)

Abstract

We examine nonlinear Beveridge curve dynamics using a globally solved Diamond-Mortensen-Pissarides model with endogenous job destruction. We theoretically establish that the Beveridge curve shifts outward when matching efficiency increases if and only if the elasticity of job separations with respect to matching efficiency exceeds the match survival rate. This condition arises because higher matching efficiency raises firms' reservation productivity, triggering *churn* that outweighs the direct effect of faster hiring. U.S. data are consistent with this state-dependent pattern, particularly in the post-pandemic period. Using the Hosios-efficient path as a benchmark, we show that endogenous separations can generate excess unemployment volatility, and that a corporate tax of about 5%—implemented as a wedge on vacancy creation—is sufficient to replicate the benchmark dynamics.

Keywords: State-dependence, Nonlinear Labor Market Dynamics, Beveridge curve, unemployment, Business Cycles.

JEL codes: E24, E32, J64

[†] The authors thank Regis Barnichon, Pawel Krolikowski, and Matthew McKernan for helpful comments and discussions. All errors are our own. Any views expressed here are solely those of the authors and do not represent those of the Bank of England or any of its committees.
Lee: hl610@cam.ac.uk. Schnattinger: Philip.Schnattinger@gmail.com.
Zanetti: francesco.zanetti@economics.ox.ac.uk

1 Introduction

The Beveridge curve—the inverse relationship between unemployment and job vacancies—is a cornerstone of macro-labor analysis. Standard search theory offers a clear prediction regarding its movements: improvements in matching efficiency should unequivocally lower unemployment for a given level of vacancies, shifting the curve inward. Yet, recent data challenges this fundamental intuition. The COVID-19 episode produced the largest Beveridge curve displacement in our sample: the outward shift averaged 0.21 log points above trend, yet the subsequent recovery, despite matching efficiency returning toward normal levels, corrected only a fraction of this displacement. More broadly, U.S. data reveal that during periods of elevated matching efficiency, the Beveridge curve shifts in response to an increase in matching efficiency *outward* rather than inward, contradicting the standard prediction. This *efficiency paradox* suggests that the forces driving labor market turnover are more complex than the canonical framework implies.

Standard macroeconomic models with exogenous job separation cannot explain this phenomenon. In these frameworks, higher matching efficiency increases the job-finding rate without affecting the separation rate, necessarily improving the unemployment-vacancy trade-off. To reconcile the model with the data, one would have to assume massive, unobserved negative shocks to other structural parameters. This inability to capture the co-movement of efficiency and unemployment inflows highlights a critical missing channel: the decision to dissolve a match is not independent of the ease of forming a new one.

In this paper, we resolve this puzzle by analyzing the Diamond-Mortensen-Pissarides (DMP) model with endogenous job destruction using a global nonlinear solution. We identify a "churning channel" that overturns standard intuition: when matching ef-

ficiency rises, the expected cost of filling a vacancy falls. This lowers the value of retaining a marginal worker, prompting firms to raise their reservation productivity and shed low-quality matches. We demonstrate that when the elasticity of this separation response is sufficiently high, it overwhelms the direct effect of faster hiring, causing the Beveridge curve to shift outward. This mechanism explains both the state-dependent reversal documented in U.S. data and the outsized, persistent Beveridge curve displacement during the COVID-19 episode, where churning dynamics slowed the recovery, without relying on ad-hoc shocks.

Beyond explaining Beveridge-curve shifts, our framework delivers a disciplined efficiency benchmark. In standard search models, the decentralized equilibrium is constrained efficient only when the Hosios condition holds pointwise. With a non-constant matching elasticity, a fixed Nash bargaining weight implies that this condition is violated away from the steady state, generating state-dependent inefficiencies in vacancy creation and, in our model, endogenous separations.

We therefore compute a *Hosios-efficient global path* by allowing the bargaining weight to adjust endogenously with tightness so that the Hosios condition holds at each date along the transition. In our calibration, the efficient benchmark has a similar mean unemployment rate to the baseline (around 4.5%) but substantially lower volatility (unemployment s.d. 8.71% vs. 10.58% in the baseline). This "efficiency gap" is largest in high matching-efficiency states, precisely when the churning channel is strongest.

Building on this benchmark, we conduct a historical analysis of unemployment dynamics by replicating two major recessions: COVID-19 and the Great Recession. We show that the outsized outward Beveridge-curve shift during the COVID-19 recovery can be accounted for by high matching efficiency interacting with endogenous job destruction, whereas the Great Recession features persistently low matching efficiency

and muted churning dynamics.

Finally, we use the efficient benchmark to evaluate simple fiscal instruments. We show that a modest corporate tax/firing penalty can substantially reduce inefficient churn and bring the baseline transition closer to the efficient path in high-efficiency episodes.

Related literature Our research is most closely related to the series of contributions by Petrosky-Nadeau and Zhang (2017, 2021), who study nonlinear dynamics in a DMP model with *exogenous* job destruction. We differ along three dimensions. First, we focus on Beveridge-curve shifts as the central object of interest in a nonlinear environment. Second, we incorporate *endogenous* job separations, which introduce cutoff-driven nonlinearities and strong state dependence. To quantify these forces reliably, we use the repeated transition method developed in Lee (2025). Third, we conduct a policy analysis relative to a Hosios-efficient benchmark. Our emphasis on nonlinear dynamics with endogenous separations is also related to Fujita and Ramey (2012). We show that the existence and shape of the implied Beveridge curve in endogenous-separation environments can be quantitatively sensitive; under our calibration and global solution, the model generates a well-defined (though shifting) negative unemployment–vacancy relationship even absent matching-efficiency shocks. This highlights the importance of calibration and nonlinear accuracy when using endogenous job destruction to study Beveridge-curve dynamics.

Beveridge curve shifts have been at the center of recent debates about the labor market and the labor market effects on inflation (Barnichon and Shapiro, 2024; Crump et al., 2024). Barlevy et al. (2024) argue that there are changing reasons for Beveridge curve shifts. We focus in this paper on shifts induced by the co-movement of matching efficiency and the separations rate increasing. These shifts are partic-

ularly interesting as they affect churn in the labor market. The Beveridge curve shifts out during these shifts as the effect of a higher separations rate induced by higher matching efficiency outweighs the inward shifting direct effect of an increase in matching efficiency. Barlevy et al. (2024) argue that this shift was prevalent during the recovery from the pandemic.

We also contribute to the literature on optimal policy in the DMP model, as discussed in Pissarides (2000). While Jung and Kuester (2015) extends this analysis to a dynamic setting, our global non-linear solution provides new insights by accurately computing higher-order moments. This precision allows us to highlight the mean-variance trade-off in firing taxes and examine how policymakers can either minimize unemployment volatility or maximize efficiency with positive firing taxes. These trade-offs arise from the impact of hiring taxes on separation and hiring rates, as well as on worker selection and productivity.

Roadmap The paper is organized as follows. Section 2 presents empirical evidence on the Beveridge curve, focusing on shifts driven by variations in matching efficiency and separation rates. Section 3 develops the model, while Section 4 details our global non-linear solution method and examines its quantitative implications for Beveridge curve shifts, state dependency, and non-linearity. We also assess the model's fit to the data. In Section 5, we introduce inefficiencies arising from wage bargaining distortions and analyze two policy tools—hiring subsidies and firing penalties—that could help restore efficiency. Finally, Section 6 concludes.

2 Motivating facts

In this section, we document two novel stylized facts that challenge standard search-and-matching theories. First, we show that the direction of Beveridge curve shifts is *state-dependent*: while matching efficiency improvements typically shift the curve inward, this relationship reverses during high-efficiency periods, generating outward shifts. Second, we find that this reversal is driven by a *positive co-movement* between matching efficiency and job separation rates. This suggests that "churn" is an endogenous response to market fluidity, a feature absent in exogenous separation models.

To establish these facts, we analyze United States data covering the period from January 1978 to June 2025. We begin by detailing the construction of our key series.

Labor market data. The vacancy rate v_t is measured using the composite Help-Wanted Index of Barnichon (2010), harmonized with JOLTS to construct a continuous vacancy series. The baseline unemployment measure u_t is the headline unemployment rate (U-3, LNS14000000, BLS). We also construct an alternative measure of unemployment that treats non-employed individuals as job seekers, defining $\tilde{u}_t = u_t + \frac{p_t^{IE}}{p_t^{UE}} i_t$, where p_t^{IE} and p_t^{UE} denote the transition probabilities from inactivity and unemployment into employment, respectively, and i_t is the inactivity rate. Our baseline separation rate is obtained from the employment-to-unemployment (EU) transition probability, seasonally adjusted using CPS microdata following Elsby, Hobijn, and Şahin (2015).[1]

[1] Appendix B describes the derivation of the transition probabilities. For robustness, we also perform the analysis using an inflow rate to unemployment accounting for transitions from both employment *and* inactivity.

Matching efficiency. We measure matching efficiency following Petrongolo and Pissarides (2001) as the residual of a standard Cobb-Douglas matching function $m_t(\mu_t, u_t, v_t) = \mu_t u_t^{\sigma} v_t^{1-\sigma}$. Dividing by unemployment yields the job-finding probability f_t, which we log-linearize as:

$$\ln f_t = \ln \bar{\mu} + (1 - \sigma) \ln(\theta_t) + \varepsilon_t, \tag{1}$$

where $\theta_t = v_t/u_t$ is labor market tightness. The fitted residual ε_t serves as our time-varying measure of matching efficiency $\ln \hat{\mu}_t$.

By construction, our measure of matching efficiency $\ln \hat{\mu}_t$ is a residual and therefore captures all movements in job-finding rates not accounted for by labor market tightness. This includes — but is not limited to — the model's structural m shock. Alternative interpretations such as worker composition shifts, mismatch, or measurement error in tightness could in principle contaminate this residual. Our empirical strategy mitigates this concern in several ways. First, by using both baseline ($\theta_t = v_t/u_t$) and alternative tightness measures ($v_t/\tilde{u}_t$), we verify that our results are not driven by a specific tightness definition. Second, the orthogonalization of ME against separations (Table 3) isolates the component of ME variation operating through separation flows specifically.

Shifts in the Beveridge curve. We derive the Beveridge curve from the standard law of motion of unemployment, $u_{t+1} = u_t + s_t - (1 - s_t) \cdot m(\mu_t, u_t, v_t)$. Solving for vacancies yields the Beveridge curve relationship $v_t = v(u_t, \mu_t, s_t, \Delta u_{t+1})$. To capture the empirical dynamics, we estimate the following log-linear specification:

$$\ln(v_t) = \beta_c + \beta_u \ln(u_t) + \beta_m \ln \hat{\mu}_t + \beta_s \ln(s_t) + \beta_{\Delta_u} \Delta \ln(\hat{u}_{t+1}) + e_t. \tag{2}$$

We define the "Beveridge curve shift" as the component of vacancies orthogonal to unemployment movements: $\ln(v_t) - \hat{\beta}_c - \hat{\beta}_u \ln(u_t) - \beta_{\Delta_u} \Delta \ln(\hat{u}_{t+1})$.

Table 1 presents the baseline results. Consistent with standard theory, the average effect of matching efficiency is to shift the curve inward ($\beta_m < 0$), while separations shift it outward ($\beta_s > 0$). However, as we show in the decomposition analysis (see Table 3 below), this average effect masks the *state-dependent reversal* described in our first stylized fact: during periods of high matching efficiency, the strong positive response of endogenous separations (the churning channel) overwhelms the direct efficiency gain, resulting in a net outward shift.

Detrending methodology. To focus on cyclical movements and isolate business-cycle dynamics from long-run structural trends in our series, we detrend the estimated Beveridge curve shifts, matching efficiencies, and separation rates using the Rotemberg (1999) filter. This filter offers an advantage over the standard HP filter: it explicitly orthogonalizes trend and cycle components by construction. This ensures that our estimated effects of matching efficiency and separations on Beveridge curve shifts are not a byproduct from spurious trend-cycle correlation mechanically induced by the HP filter, but rather reflect genuine cyclical labor market dynamics independent of any low-frequency structural changes. Our headline results also hold when detrending with Hodrick–Prescott Hodrick and Prescott (1997) filters (see Appendix B) or when variables are regressed in levels; these robustness checks are reported in Appendix B.

Figure 1 presents the detrended cyclical components of the Beveridge curve shifts (left panel), matching efficiency (center panel), and separation rate (right panel) for both baseline and alternative measures. The baseline measures use employment-to-unemployment (E→U) flows and standard labor market tightness (v_t/u_t), while the al-

Table 1: Beveridge curve regressions

	Specification		
	(1)	(2)	(3)
Dependent Var.: Vacancy Rate v_t	**Baseline**	**Without controls**	**With inactive searchers**
Matching efficiency	-1.096***		-0.864***
	(0.090)		(0.091)
Separation rate (s_t)	1.041***		1.126***
	(0.090)		(0.093)
Unemployment (u_t)	-1.234***	-0.628***	-0.867***
	(0.058)	(0.032)	(0.035)
$\Delta \ln u_{t+1}$	-2.774***	-0.602***	-2.121***
	(0.224)	(0.151)	(0.180)
Constant	✓	✓	✓

Note: Monthly U.S. data from January 1978 to June 2025. The dependent variable is the log vacancy rate. Column (1) presents the baseline specification including matching efficiency and the separation rate as control variables in addition to log unemployment and the one-month-ahead change in log unemployment. Column (2) excludes matching efficiency and separations, reporting only the raw relationship between vacancies and unemployment. Column (3) uses separation and matching efficiency measures which account for inactive job seekers. Matching efficiency is constructed as the residual from a log matching-function regression of the job-finding rate on labor-market tightness (with column (3) using a generalized tightness measure based on effective searchers). The separation rate is constructed from CPS-based continuous-time adjusted transition hazards (employment into unemployment in columns (1) and (2); a broader measure combining separations from employment and nonparticipation in column (3)). Standard errors are conventional i.i.d. OLS standard errors. Significance levels: *** $p < 0.01$, ** $p < 0.05$, * $p < 0.10$.

ternative measures incorporate combined employment and inactivity-to-unemployment (E∪N→U) flows and effective-searcher tightness ($v_t/\tilde{u}_t$) to account for job search by the inactive. These detrended series capture the cyclical movements in the Beveridge curve originating from matching efficiency and the separation rate, represented by the terms $\beta_m \ln(\hat{\mu}_t)$ and $\beta_s \ln(\hat{s}_t)$, respectively, as well as unexplained movements due to the error term e_t in equation (2). The figure illustrates that both measurement approaches yield qualitatively similar cyclical patterns, reinforcing the robustness of our findings.

To complement the cyclical analysis in Figure 1, we construct Figure 2, which displays 13-month centered moving averages of the *level* series (i.e., without detrending) of Beveridge curve shifts, matching efficiency, and separations. This moving average smoothing removes high-frequency noise while preserving both cyclical and trend movements, making it easier to identify major shift episodes and their duration. Whereas Figure 1 isolates business-cycle fluctuations by removing low-frequency trends, Figure 2 retains these longer-run movements and highlights the six largest shift intervals identified in Table 2 with colored segments.

Table 2 identifies the six largest shift episodes by searching the Rotemberg-detrended series for contiguous intervals in which the cyclical component of the Beveridge curve shift exceeds ± 0.5 standard deviations. The table reports the mean deviation of the BC shift from its trend during each interval (column 1), together with the corresponding mean deviations of matching efficiency (column 2) and the job separation rate (column 3). The largest outward-shift episode in our sample is January 2019–September 2022, which spans the onset of the COVID-19 pandemic and the early recovery, with a mean cyclical deviation of +0.21. The subsequent inward shift during October 2023–June 2025 (-0.23) reflects the normalization of the labor market. Other notable episodes include the post-Great Recession period January 2010–August 2013 (+0.19), the pre-pandemic tightening September 2016–October 2018 (-0.19), and two earlier episodes in November 1990–February 1992 (-0.15) and August 2000–November 2000 (-0.15).

According to our estimates in Table 1, on average across the full sample period, improvements in matching efficiency shift the Beveridge curve inward, while increases in the job separation rate shift it outward. However, the entries in Table 2 reveal a more nuanced pattern for the largest shift episodes. Specifically, outward shifts are predominantly associated with above-trend separations (e.g., +0.10 in Jan 2019–Sep

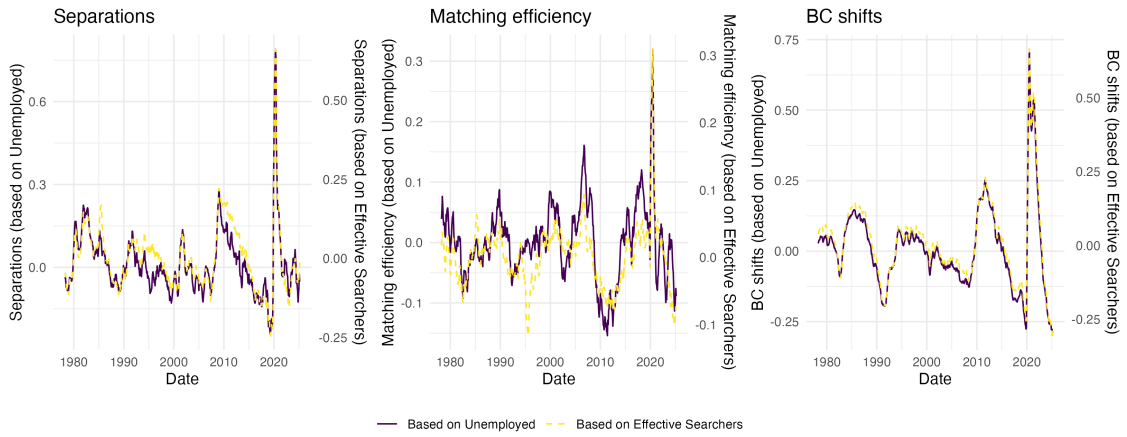

Figure 1: Detrended Beveridge curve shifts, matching efficiency, and separation rates

Note: This figure displays the cyclical components of Beveridge curve shifts (left panel), matching efficiency (center panel), and separation rates (right panel), detrended using the Rotemberg (1999) filter. Each panel shows two series: (i) *Baseline* measures computed using employment-to-unemployment (E→U) flows and standard tightness (v_t/u_t), and (ii) *Alternative* measures computed using combined employment *and* inactivity-to-unemployment (E∪N→U) flows and effective-searcher tightness ($v_t/\tilde{u}_t$), where $\tilde{u}_t$ includes inactive job seekers weighted by their job-finding rates relative to the unemployed. The detrending isolates business-cycle fluctuations from long-run structural trends. Sample period: Jan 1978 to Jun 2025. Data source: FRED, JOLTS, and CPS.

2022, +0.07 in Jan 2010–Aug 2013), while inward shifts tend to coincide with below-trend separations (e.g., −0.10 in Sep 2016–Oct 2018, −0.12 in Aug 2000–Nov 2000). The November 1990–February 1992 episode is notable as an exception, exhibiting an inward shift alongside above-trend separations (+0.08), consistent with the early 1990s recession driving separations higher even as the curve moved inward. Overall, these results reinforce the central role of separation rate dynamics in driving the largest Beveridge curve shifts.

We next decompose the channels through which matching efficiency and job separations affect Beveridge curve shifts. A key insight from our theoretical framework is that matching efficiency can induce endogenous separations: higher matching efficiency reduces the expected cost of filling a vacancy, encouraging firms to create jobs but also lowering the value of marginal matches, potentially triggering more job destruction. To isolate these two channels empirically, we decompose the total effect

Figure 2: Beveridge curve shifts over time.

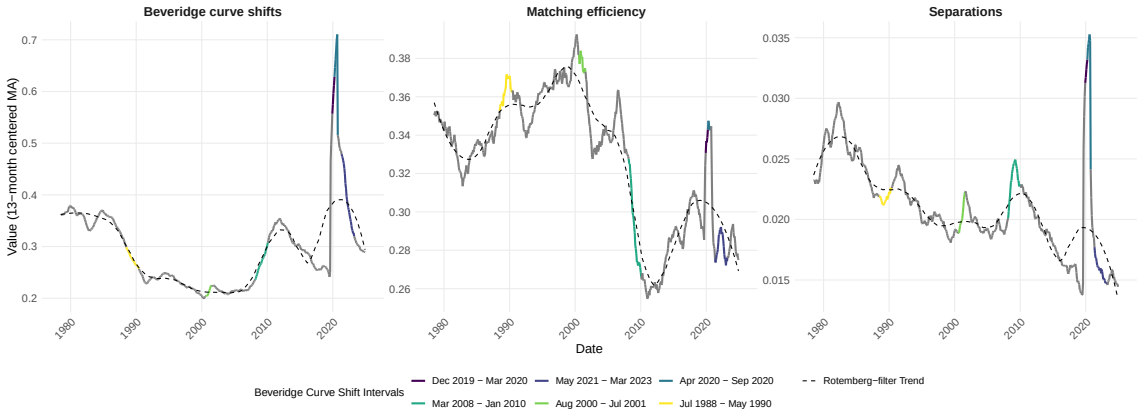

Note: This figure shows 13-month centered moving averages of Beveridge-curve shifts, matching efficiency, and separations from Jan 1978 to Jun 2025. The smoothing helps reveal underlying trends by reducing high-frequency noise. The colored segments highlight the top 6 shift intervals identified in the table, with each color corresponding to a specific interval. Gray segments indicate periods outside these major shift episodes. The three panels display (left to right): BC shifts computed as deviations in the vacancy-unemployment relationship, matching efficiency, and separation rates. Data source: FRED, JOLTS, and CPS.

of matching efficiency into (i) the component that operates through induced separations, and (ii) the residual component orthogonal to separations, which captures the direct matching effect holding separations constant. This decomposition is implemented via a first-stage regression of matching efficiency on separations (including CPS inactivity-flow controls), with the fitted values capturing the endogenous separation channel and the residuals capturing the orthogonalized matching efficiency channel. The first-stage regression results are reported in Appendix B.

Table 3 presents regression results examining how matching efficiency and job separations affect Beveridge curve shifts. Columns (1) and (2) report results for the full sample, while columns (3) and (4) restrict attention to periods when matching efficiency exceeds the 67th percentile (i.e., high matching efficiency periods). Columns (1) and (3) regress BC shifts on matching efficiency alone, while columns (2) and (4) implement the channels decomposition, separating the total effect into the endogenous separation channel and the orthogonalized matching efficiency channel.

Table 2: Top Beveridge-curve shift intervals

Interval	**BC shift** (mean dev., log pts)	**Matching efficiency** (mean dev., log pts)	**Separations** (mean dev., log pts)
Oct 2023–Jun 2025	-0.23	-0.04	-0.03
Jan 2019–Sep 2022	0.21	0.04	0.10
Sep 2016–Oct 2018	-0.19	0.08	-0.10
Jan 2010–Aug 2013	0.19	-0.11	0.07
Nov 1990–Feb 1992	-0.15	0.01	0.08
Aug 2000–Nov 2000	-0.15	0.07	-0.12

Note: This table presents the top 6 Beveridge-curve shift intervals, ranked by the absolute mean deviation of the Rotemberg-detrended BC shift from its trend. Each interval is a contiguous period where the cyclical component of the BC shift exceeds ±0.5 standard deviations. All columns report mean deviations from the Rotemberg trend (in log points): BC shift (`bc_shift1_cps_flow_rotcyc`), matching efficiency (`meff5_AC_rotcyc`), and separations (`lsep_flow_cps_rotcyc`). Sample: Jan 1978 to Jun 2025. Data source: FRED, JOLTS, and CPS.

The full-sample results in column (1) show that matching efficiency exhibits a negative coefficient (-0.261), consistent with the standard view that improvements in matching efficiency shift the Beveridge curve inward. The channels decomposition in column (2) reveals that separations have a positive coefficient (0.613), shifting the curve outward, while matching efficiency orthogonalized to separations has a negative coefficient (-0.467). However, columns (3) and (4) reveal a striking reversal during high matching efficiency periods. Column (3) shows that the overall matching efficiency effect becomes positive (0.424), implying that increases in matching efficiency shift the Beveridge curve *outward* rather than inward during these periods. Column (4) demonstrates that this reversal occurs because the endogenous separation channel (captured by the separations coefficient of 0.605) dominates the direct matching effect (captured by the orthogonalized matching efficiency coefficient of -0.112), highlighting the critical role of endogenous separation dynamics in driving Beveridge curve shifts during periods of elevated matching efficiency.

Table 3: Beveridge curve shifts, matching efficiency, and job separation

	Beveridge Curve Shifts		Beveridge Curve Shifts when ME $\geq$ 67th pctile(ME)	
	(1) Matching Efficiency	(2) Channels	(3) Matching Efficiency	(4) Channels
Matching Efficiency	-0.261***		0.424***	
	(0.080)		(0.134)	
Separations		0.613***		0.605***
		(0.034)		(0.065)
Matching Efficiency orthogonalized to Separations		-0.467***		-0.112
		(0.063)		(0.128)
Constant	-0.449***	-0.306***	-0.592***	-0.597***
	(0.107)	(0.078)	(0.160)	(0.140)
Observations	570	570	190	190

Note: Monthly U.S. data from January 1978 to June 2025. The dependent variable is the Beveridge curve shift. Columns (1) and (3) report regressions of BC shifts on matching efficiency. Columns (2) and (4) report the channels decomposition: BC shifts regressed on separations and matching efficiency orthogonalized to separations. Columns (1)–(2) use the full sample, while columns (3)–(4) restrict to periods of large shifts, defined as observations where matching efficiency exceeds the 67th percentile (i.e., high matching efficiency periods). All variables are standardized. The decomposition is implemented via a first-stage regression of matching efficiency on separations (including CPS inactivity-flow controls), with the fitted values capturing the endogenous separation channel and the residuals capturing the orthogonalized matching efficiency channel. The second-stage regressions control for log unemployment and CPS inactivity-flow transitions (p_{UN}, p_{NU}, p_{EN}, p_{NE}); coefficients on these controls are suppressed. Standard errors are conventional i.i.d. OLS standard errors. Significance levels: *** $p < 0.01$, ** $p < 0.05$, * $p < 0.10$.

To summarise, in this section we have shown that the Beveridge curve typically shifts inward when matching efficiency increases. However, the shift direction is non-linear and state-dependent. When matching efficiency increases are accompanied by separation rate increases, the Beveridge curve shifts outward. In the following sections, we show how a standard non-linearly and globally solved DMP model with endogenous job destruction in the spirit of Mortensen and Pissarides (1994) can capture these features and their implications.

3 Theoretical framework

Definition 1 (Beveridge curve)**.**

Fix a reduced-form mapping from matching efficiency m to the gross separation rate, denoted $s^\star(m) \in (0,1)$. The Beveridge curve is the locus $B(m)$ of unemployment–vacancy pairs $(u,v) \in \mathbb{R}_+ \times \mathbb{R}_+$ satisfying

$$\frac{M(u,v)}{1-u} = \frac{1}{m}\frac{s^\star(m)}{1-s^\star(m)}. \tag{3}$$

Equation (3) nests the canonical Beveridge curve. In standard models with exogenous separations, $s^\star(m)$ is constant, while in models with endogenous job destruction, $s^\star(m)$ inherits equilibrium feedback through the job-destruction cutoff and market tightness.

Rearranging (3) yields

$$\frac{M(u,v)}{1-u} = \frac{1}{m}\frac{s^\star(m)}{1-s^\star(m)} = -\frac{1}{m} + \frac{1}{m(1-s^\star(m))}. \tag{4}$$

Since the left-hand side is strictly increasing in v for any fixed u, an increase in the right-hand side corresponds to an outward shift of the Beveridge curve (higher v required to support a given u).

Differentiating the right-hand side with respect to m yields the decomposition

$$\frac{\partial}{\partial m}\left(-\frac{1}{m} + \frac{1}{m(1-s^\star(m))}\right) = -\frac{1}{m^2}\frac{s^\star(m)}{1-s^\star(m)} + \frac{1}{m(1-s^\star(m))^2}\frac{ds^\star(m)}{dm}, \tag{5}$$

where the first term is the *direct hiring effect* and the second term is the *endogenous churning effect*.

Theorem 1 (Condition for outward shifts)**.**

An increase in matching efficiency shifts the Beveridge curve outward if and only if

$$\frac{d\log s^\star(m)}{d\log m} > 1 - s^\star(m). \tag{4}$$

Proof. Define $B(m) \equiv -\frac{1}{m} + \frac{1}{m(1-s^\star(m))}$. An outward shift is equivalent to $dB(m)/dm > 0$. Differentiating $B(m)$ and rearranging yields that $dB(m)/dm > 0$ if and only if

$$\frac{1}{1-s^\star(m)}\frac{ds^\star(m)}{dm} > \frac{s^\star(m)}{m}. \tag{5}$$

Multiplying both sides by $m/s^\star(m)$ gives

$$\frac{d\log s^\star(m)}{d\log m} > 1 - s^\star(m). \tag{6}$$

■

When m increases, the expected cost of filling a vacancy falls, increasing the firm's outside option. Consequently, firms become more selective, raising the reservation productivity threshold. If the density of matches near this threshold is high, the resulting surge in separations, captured by the elasticity term in Theorem 1, overwhelms the faster hiring speed. This result explains the "efficiency paradox" observed in post-COVID data: the labor market was highly fluid, but this very fluidity encouraged a rate of labor turnover that kept unemployment elevated relative to vacancies.

In our quantitative environment, $s^\star(m)$ is endogenously induced by the equilibrium reservation-productivity cutoff and tightness; Sections 5 quantify the state-dependent elasticity $d\log s^\star(m)/d\log m$ and show that it exceeds the threshold in high-efficiency states in the calibrated model.

Corollary 1 (Exogenous separation)**.**

If separations are exogenous, $s^{\star}(m)$ is constant in m and the Beveridge curve shifts inward when m increases.

Proof. In the exogenous job separation model, the separation rate is constant, so $\frac{\partial \log(s^*(m))}{\partial \log(m)} = 0$. This implies that the elasticity of the job separation rate with respect to matching efficiency is always lower than the survival rate, and the condition in Theorem 1 never holds. ■

Corollary 1 provides a useful benchmark. If separations do not respond to matching efficiency, then the churning margin is shut down: improvements in m only speed up job creation, without inducing additional job destruction. In that case, the Beveridge curve shifts inward unambiguously. The corollary thus highlights that the sign reversal documented in the data—and rationalized in our model—requires separations to endogenously co-move with matching conditions.

4 Baseline model

Our model formulation is consistent with the most commonly employed versions of the Diamond-Mortensen-Pissarides Model formulated in (Mortensen and Pissarides, 1994; Den Haan, Ramey, and Watson, 2000; Yashiv, 2007; Hagedorn and Manovskii, 2008). Time is discrete. Firms produce outputs only using labor inputs. The firms post vacancies to be matched with unemployed workers in a labor market characterized by search frictions.

Timing Within period $t-1$, a fraction λ of existing matches is destroyed exogenously, sending displaced workers into unemployment. Unemployed workers then

search and firms post vacancies; matching occurs within period $t-1$. Matches formed in $t-1$ become active at the beginning of period t. At the start of period t, firms observe match productivity and endogenously destroy matches below the reservation threshold $z_s(S)$. Surviving matches then bargain over wages and produce in period t. The timing is summarized in Figure 3.

Figure 3: Timing in the model

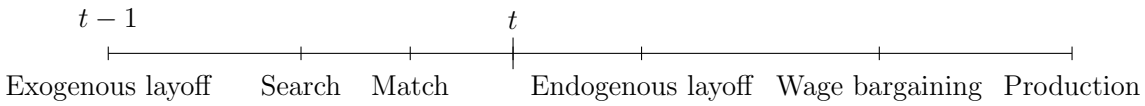

Notes: In period $t-1$, an exogenous shock destroys a fraction λ of existing matches. Unemployed workers then search and match with vacancies within $t-1$, forming matches that become active at the start of t. At the start of t, firms observe match productivity and endogenously destroy matches below the reservation threshold z_s. Surviving matches bargain wages and produce.

Matching function Following Den Haan, Ramey, and Watson (2000), we consider the following CRS matching function:[2]

$$M(V,U) = \frac{UV}{(V^{\xi}+U^{\xi})^{\frac{1}{\xi}}} \ . \tag{7}$$

The number of new matches $m \times M$ in the economy is determined by the number of vacancies V posted by firms, the number of unemployed workers U searching to fill these vacancies, and matching efficiency m. Based on the matching function, we define the job finding rate p and vacancy filling rate q as follows:

$$p(\theta) := m\theta(1+\theta^{\xi})^{-\frac{1}{\xi}} \tag{8}$$

$$q(\theta) := m(1+\theta^{\xi})^{-\frac{1}{\xi}}, \tag{9}$$

[2]We also consider a Cobb-Douglas CRS matching function as a robustness check for our main results, which does not change significantly from the baseline.

where $\theta := \frac{V}{U}$ is the market tightness.

Aggregate states The aggregate states S are composed of exogenous and endogenous parts. The exogenous component is the aggregate TFP level A and the matching efficiency m. The endogenous part is the prior period's incumbent and newly matched workers n^*_{-1}.

$$S = \left\{A, m, n^*_{-1}\right\} \tag{10}$$

The log aggregate TFP follows an AR(1) process:

$$log(A') = \rho_A log(A) + \sigma_A \epsilon, \quad \epsilon \sim_{iid} N(0,1). \tag{11}$$

The log aggregate matching efficiency also follows an AR(1) process:

$$log(m') = (1-\rho_m) log(\overline{m}) + \rho_m log(m) + \sigma_m \epsilon, \quad \epsilon \sim_{iid} N(0,1), \tag{12}$$

where $\overline{m}$ is the unconditional average the matching efficiency. The current working population n is endogenously determined by the following law of motion:

$$n(S) = (1-\lambda)(1-H(S))(n^*_{-1}) \tag{13}$$

$$n^*(S) = n(S) + v(S) q(\theta(S)) \tag{14}$$

where λ is the exogenous separation rate. $H(S)$ is the endogenous separation rate set by firms' endogenous job destruction decisions.

Household We consider a representative household that is composed of a contin-

uum of unit measures of labor forces. The employed portion of the labor force earns wages, and the unemployed portion engages in home production, all of which are treated as labor income $W(S)$. The household holds the claim for the dividend $D(S)$ and saves for future dividend claims. Thus, the budget constraint is as follows:

$$c + a' = W(S) + D(S) + \underbrace{(a - D(S))}_{\text{Ex-dividend equity value}} \tag{15}$$

where a is the value of the dividend claim. The apostrophe indicates the future variables. The household has a temporal CRRA utility and discounts future by $\beta \in (0, 1)$. The recursive formulation of the households' problem is as follows:

$$V(a; S) = \max_{c,a'} \quad \frac{c^{1-\sigma}}{1-\sigma} + \beta \mathbb{E} V(a'; S') \tag{16}$$

$$\text{s.t.} \quad c + a' = W(S) + D(S) + (a - D(S)) \tag{17}$$

Real values of employment and unemployment A continuum of a unit measure of ex-ante homogenous labor force is considered. Their labor productivity z is distributed as follows:

$$z \sim_{iid} N(1, \sigma_z) \tag{18}$$

Matched individuals get a new productivity drawn in every period. When a worker is employed, they earn wage. Then, an exogenous Poisson separation shock arrives at a rate of $\lambda \in (0, 1)$. The worker continues to stay in the match in the following period with a probability of $(1 - \lambda)$ or searches for another job with probability λ and gets matched with a new job with a probability of $p = p(\theta(S))$. In the following period, a firm decides whether to lay off the worker, which is captured by endogenous separation

rate $H(S')$. All workers are assumed to participate in job search when unemployed. All the future values are discounted by the stochastic discount factor $\mu(S, S')$. In equilibrium, the wage is determined by Nash bargaining, resulting in $w = w(z; S)$. We define the value function of an employed worker earning the equilibrium wage $v^e(z; S)$ and the value function of an unemployed worker $v^u(z; S)$ as follows:

$$
\begin{aligned}
v^e(z;S) &= w(z;S) \\
&+ ((1-\lambda) + \lambda p(\theta(S)))\mathbb{E}\left[\mu(S,S')(1-H(S'))(v^e(z';S') - v^u(z';S'))\middle| J(z';S') > 0\right] \\
&+ \mathbb{E}\left[\mu(S,S')v^u(z';S')\right] \qquad (19) \\
v^u(z;S) &= b + p(\theta(S))\mathbb{E}\left[\mu(S,S')(1-H(S'))(v^e(z,w';S') - v^u(z';S'))\middle| J(z';S') > 0\right] \\
&+ \mathbb{E}\left[\mu(S,S')v^u(z';S')\right] \qquad (20)
\end{aligned}
$$

When a worker starts a period as unemployed, the worker engages in home production $b > 0$ and searches for a job to be matched with a vacancy with the probability $p = p(\theta(S))$.

Firms (=jobs) A firm (job) produces output using a CRS Cobb-Douglas function with only a labor input.[3] In equilibrium, the wage is determined as $w = w(z; S)$ by Nash bargaining. Based on this, we define the value function J of a firm that pays out the equilibrium wage, $J(z; S)$:

$$J(z;S) = Az - w(z;S) + (1-\lambda)\mathbb{E}\left[\mu(S,S')(1-H(S'))J(z';S')|J(z';S') > 0\right] \qquad (21)$$

where $\mu(S, S')$ is the stochastic discount factor. At the beginning of a period, a firm

[3]The CRS production allows the firm-level characterization to boil down to the job-level characterization as in other models in the literature.

decides whether to destruct a job based on the following individual rationality condition: $J(z;S) > 0$. It is worth noting that all the value functions are written at the timing after the job destruction decision, which eases the wage bargaining characterization. We define the endogenous job destruction probability $H(S)$ accordingly:

$$H(S) := \mathbb{P}\left(J(z;S) < 0\right). \tag{22}$$

Wage bargaining A matched worker with productivity z and the firm determine the wage by Nash bargaining. The worker's bargaining power is $\eta > 0$. The standard Nash bargaining leads to the following condition where the wage is determined:

$$(1-\eta)(v^e(z;S) - v^u(z;S)) = \eta J(z;S) \tag{23}$$

Detailed derivation of this condition is available in the Appendix.

Equilibrium conditions In equilibrium, we require the following conditions:

$$\text{[Free entry]} \quad \kappa = q(\theta(S))(1-\lambda)\mathbb{E}\left[\mu(S,S')(1-H(S'))J(z';S')|J(z';S') > 0\right] \tag{24}$$

$$\text{[Agg. output]} \quad Y(S) = A\int_{J(z;S)>0} z d\Phi + b\int_{J(z;S)\leq 0} d\Phi \tag{25}$$

$$\text{[Resource const.]} \quad C(S) = Y(S) - \kappa v(S) = W(S) + D(S) \tag{26}$$

The first is free entry conditions. Firms pay a cost κ when they post a vacancy. In equilibrium, a firm's expected profit and the vacancy posting cost balance. In the national account, aggregate output Y balances with the aggregate consumption C after accounting for the total vacancy posting cost. From the income side identity, the consumption is equal to the sum of labor and capital (dividend) incomes minus

the lump-sum tax.

4.1 Equilibrium characterization

We characterize the equilibrium by establishing the values for wages, job creation, and crucially, the endogenous job destruction threshold.

Wage Determination. Wages are determined via Nash bargaining, sharing the surplus of the match according to the worker's bargaining power η. Using the value functions defined above, the bargaining condition $(1-\eta)(v^e(z)-v^u(z)) = \eta J(z)$ yields the equilibrium wage schedule:

$$w(z;S) = (1-\eta)b + \eta(Az + \theta\kappa). \tag{27}$$

The wage is a weighted average of the worker's outside option (home production b) and the match productivity plus labor market tightness benefits.

Endogenous "churning" threshold The core mechanism of our model lies in the firm's decision to dissolve a match. A firm destroys a job if the match value becomes negative, $J(z;S) < 0$. This defines a reservation productivity threshold $z_s(S)$ where the firm is indifferent between retaining the worker and separating:

$$z_s(S) = \frac{1}{A}\left(\underbrace{b + \frac{\eta}{1-\eta}\theta\kappa}_{\text{Outside Options}} - \underbrace{\frac{1}{1-\eta}\frac{\kappa}{q(\theta(S))}}_{\text{Hoarding Value}}\right). \tag{28}$$

Equation (28) reveals the economic trade-off governing separations. The threshold z_s increases with the worker's outside option b and market tightness θ. Crucially, it decreases with the expected hiring cost $\frac{\kappa}{q(\theta)}$. When hiring is costly (low $q(\theta)$), firms "hoard" labor, tolerating lower productivity matches (lower z_s). Conversely, when matching becomes efficient (high m, high $q(\theta)$), the cost of replacing a worker falls. This reduces the hoarding motive, raising z_s and triggering "churn."

Based on this threshold, the endogenous separation rate is the mass of employment below the cutoff:

$$H(S) = \Phi\left(\frac{z_s(S) - 1}{\sigma_z}\right). \tag{29}$$

Job creation condition. Firms post vacancies until the expected cost equals the expected benefit. The benefit depends on the expected surplus from a new hire, which is conditional on the new match surviving the endogenous separation cut in the next period $(1 - H(S'))$:

$$\frac{\kappa}{q(\theta(S))} = (1-\lambda)\mathbb{E}\left[\mu(S,S')(1-H(S'))J(z';S') \mid J(z';S') > 0\right]. \tag{30}$$

Substituting the wage equation (27) into the value function $J(z)$, we obtain the fundamental Job Creation (JC) condition:

$$\frac{\kappa}{q(\theta(S))} = (1-\lambda)\mathbb{E}\left[\mu(S,S')(1-H(S'))\left((1-\eta)(A'\overline{z}(S') - b) - \eta\theta(S')\kappa + \frac{\kappa}{q(\theta(S'))}\right)\right], \tag{31}$$

where $\overline{z}(S') = \mathbb{E}[z|z > z_s(S')]$ is the average productivity of surviving matches.

Table 4 summarizes the full dynamic system governing the economy.

Description	Equation
Aggregate productivity	$\log(A') = \rho_A \log(A) + \sigma_A \epsilon$
Aggregate matching efficiency	$\log(m') = \rho_m \log(m) + \sigma_m \epsilon$
Endogenous Job destruction	$H = \Phi(\frac{z_s - 1}{\sigma_z})$
Matches at the start of the period	$n^* = n + vq(\theta)$
Law of motion of employment	$n = (1-\lambda)(1-H)n^*_{-1}$
Job creation condition	$\frac{\kappa}{q(\theta)} = (1-\lambda)\mathbb{E}[\mu(1-H')\left(A'\overline{z}' - \overline{w}' + \frac{\kappa}{q(\theta')}\right)]$
Job destruction condition	$Az_s = b + \frac{\eta}{1-\eta}\kappa\theta - \frac{1}{1-\eta}\frac{\kappa}{q(\theta)}$
Cond. mean match productivity	$\overline{z} = 1 + \sigma_z \frac{\phi(\frac{z_s-1}{\sigma_z})}{1-\Phi(\frac{z_s-1}{\sigma_z})}$
Bargained average wage	$\overline{w} = (1-\eta)b + \eta[A\overline{z} + \theta\kappa]$
Probability of finding a job	$p(\theta) = m\theta(1+\theta^\xi)^{-\frac{1}{\xi}}$
Probability of filling a vacancy	$q(\theta) = m(1+\theta^\xi)^{-\frac{1}{\xi}}$
Resource constraint	$C = A\overline{z}n + b(1-n) - \kappa v$
Stochastic discount factor	$\mu = \beta\left(\frac{C'}{C}\right)^{-\sigma}$
Tightness	$\theta = \frac{v}{u}$
Unemployed	$u = 1 - n$

Table 4: Summary of assumptions and equilibrium conditions

Notes: This table summarizes the equilibrium conditions in the baseline model.

4.2 The anatomy of the separation elasticity

We now connect the equilibrium conditions to the "Churning Channel" identified in Theorem 1. The theorem states that the Beveridge curve shifts outward if the elasticity of separations to matching efficiency is sufficiently high. Here, we derive the structural form of this elasticity.

Proposition 1 (Transmission mechanism)**.**

Holding market tightness θ fixed, an increase in matching efficiency m raises the

reservation productivity threshold z_s.

$$\frac{\partial z_s(S)}{\partial m} > 0. \tag{32}$$

Proof. An increase in m raises the vacancy filling rate $q(\theta)$ for any given θ. From the Job Destruction condition (28), a higher q reduces the expected hiring cost term ($-\frac{\kappa}{q}$ becomes less negative), directly increasing z_s. ■

This proposition confirms the intuition that easier hiring reduces labor hoarding. We can now quantify the separation elasticity $\varepsilon_{s,m}$ that governs the Beveridge curve shift. Differentiating the gross separation rate $s(m) = 1 - (1-\lambda)(1-\Phi(z_s))$, we obtain:

$$\underbrace{\frac{\partial \log s(m)}{\partial \log m}}_{\text{Elasticity } \varepsilon_{s,m}} = \underbrace{\left(\frac{(1-\lambda)\phi_z(\hat{z}_s)}{s(m)}\right)}_{\text{Density at Cutoff}} \times \underbrace{\left(\frac{\partial z_s}{\partial m}\frac{m}{\sigma_z}\right)}_{\text{Sensitivity of Cutoff}}. \tag{33}$$

Equation (33) reveals why the Beveridge curve shift is non-linear and state-dependent. The magnitude of the "churning" response depends on the density of matches at the cutoff, $\phi_z(\hat{z}_s)$. In general equilibrium, θ adjusts with m. Section 5 verifies numerically that the total effect of higher m on z_s is positive in the high-efficiency states that drive the outward shifts.

As shown in Figure 4, this density is not constant. When the economy is in a state where z_s falls into a high-density region of the productivity distribution (the "Upward shift region"), a small improvement in matching efficiency triggers a disproportionately large wave of separations. Since productivity shocks are normally distributed, the density ϕ_z is hump-shaped. This implies that the 'churning channel' is most po-

Figure 4: Beveridge curve shifts and the matching efficiency cutoffs

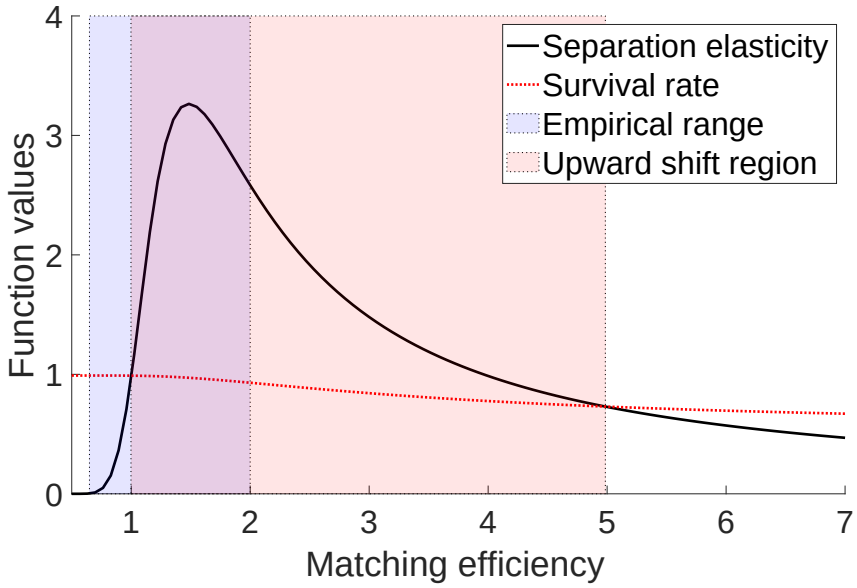

Notes: The figure illustrates the condition from Theorem 1. The black line represents the separation elasticity $\varepsilon_{s,m}$. When this elasticity exceeds the survival rate (red dotted line), the Beveridge curve shifts outward.

tent when the reservation threshold z_s is near the center of the distribution—exactly where the economy sits during high-efficiency recoveries. This structural feature explains why the Beveridge curve response can flip from inward to outward depending on the state of the economy.

5 Quantitative analysis

5.1 Solution method

The canonical endogenous job destruction model displays highly nonlinear global unemployment dynamics due to the endogenous destruction cutoff change in the cross-sectional skill distribution. Agents form a consistent expectation of the future dynamics to make a contemporaneous decision. In the baseline model, one of the

important channels where the expectation plays a key role is the vacancy posting condition, where the state-contingent marginal benefit of vacancy posting needs to be computed. Therefore, it is necessary to sharply characterize the nonlinear functional form of the aggregate states to solve the global solution recursive competitive equilibrium globally. This difficulty has limited the global analysis of the impact of endogenous separation on the labor market dynamics. The recent global solution method, the repeated transition method by Lee (2025), overcomes this problem in the sequence space by utilizing the recursivity of the recursive competitive equilibrium. Specifically, it utilizes the fact that all the recursive competitive equilibrium outcomes are realized on a simulated exogenous shock path if the simulated path is long enough, forming an ergodic set of all the possible aggregate allocations. Then, by identifying and combining the last iteration's value (policy) functions of the period with the aggregate states realized to be closest to the future states, the conditional expectation can be accurately computed in each period. The detailed implementation is elaborated in the Appendix.

A key quantitative object in our analysis is the global equilibrium path implied by the Hosios condition, which we use as an efficient benchmark for the baseline economy. With a CES matching function, the Hosios condition requires the worker's bargaining weight to vary with market tightness over the cycle, which turns the computation of the benchmark into a fixed-point problem in sequences. We compute this benchmark using the repeated transition method, which iterates jointly on the sequence of bargaining weights and the associated equilibrium allocations until convergence. Section 5 compares the Hosios benchmark to the baseline model and studies how standard policy wedges can replicate benchmark dynamics in high-efficiency states.

5.2 Calibration Strategy

We calibrate the model at a monthly frequency to match key first and second moments of the U.S. labor market. Our strategy distinguishes between standard structural parameters, which are set to values common in the literature, and mechanism-specific parameters, which are calibrated to match the volatility of unemployment and vacancies.

Table 5 summarizes the parameter values. Parameters marked with an asterisk (*) are internally calibrated to minimize the distance between model-generated moments and their empirical counterparts; parameters marked with a dagger (†) are externally estimated and held fixed during the internal calibration.

Standard parameters. We set the discount factor β to match an annualized interest rate of 4%. The matching function elasticity ξ is set to 0.7, consistent with standard estimates. The exogenous separation rate λ is fixed at 0.01, attributing the remainder of labor turnover to the endogenous channel.

Targeted moments and identification. Table 6 reports the target moments used to discipline the model's dynamic behavior. We construct the empirical moments using U.S. data extended from 1955 to 2024. Vacancies are measured using the composite Help-Wanted Index (Barnichon, 2010), harmonized with JOLTS data. Unemployment and job-finding rates are constructed from BLS data following the methodology of Shimer (2005).

The calibration of the shock processes is critical for the quantitative analysis. We employ a two-step approach:

1. **Matching efficiency process (external estimation):** We first estimate the stochastic process for matching efficiency (ρ_m, σ_m) directly from the data using

Table 5: Calibrated Parameters

Parameters	Description	Value
Basic parameters		
b	Unemployment benefit*	0.5018
κ	Vacancy posting cost*	0.7993
m	Average matching efficiency*	1.3743
σ_z	Idiosyncratic productivity dispersion*	1.1000
λ	Exogenous separation rate	0.0100
ξ	Matching function parameter	0.7000
β	Household's discount factor	0.9966
η	Worker's bargaining power	0.4455
Aggregate shock parameters		
ρ_A	Aggregate productivity shock persistence	0.9830
σ_A	Aggregate productivity shock volatility*	0.0330
ρ_m	Matching efficiency shock persistence†	0.9770
σ_m	Matching efficiency shock volatility†	0.0400

Note: This table reports the calibrated parameter levels. Parameters marked with an asterisk (*) are jointly calibrated to match the targets in Table 6. Parameters marked with a dagger (†) are externally estimated from the data and held fixed during the joint calibration.

a Kalman filter, following Sedláček (2014). This treats matching efficiency as an unobserved component driving the wedge in the matching function, identified by variations in the vacancy, unemployment, and hire rates. The resulting estimates are fixed at their Kalman-filter values and are not adjusted in the subsequent step.

2. **TFP and productivity dispersion (internal calibration):** Conditional on the estimated matching efficiency process, we calibrate the TFP volatility σ_A and the idiosyncratic productivity dispersion σ_z to match the observed volatilities of unemployment and vacancies.

Crucially, the idiosyncratic dispersion parameter σ_z determines the shape of the productivity distribution $F(z)$. By governing the density of matches near the reservation threshold z_s, σ_z dictates the sensitivity of endogenous separations to aggregate shocks. A precise calibration of this parameter is therefore essential to capture the "churning channel" accurately. We solve the model globally by discretizing the TFP process into 11 grid points (covering ± 3 standard deviations) and the matching efficiency process into 3 grid points (covering ± 1 standard deviation) using the Tauchen method.

Table 6: Calibration Targets vs. Model Moments

	Model	Data	Reference
Steady-state			
Unemployment rate u_{ss}	0.050	0.050	Bureau of Labor Statistics (BLS)
Vacancy posting rate v_{ss}	0.037	0.037	Bureau of Labor Statistics (BLS)
Job-finding rate p_{ss}	0.433	0.433	Bureau of Labor Statistics (BLS)
Business cycle			
Unemp. volatility $s.d.(u_t)$ $(p.q.$ in $\%)$	10.584	11.400	Bureau of Labor Statistics (BLS)
Vacancy volatility $s.d.(v_t)$ $(p.q.$ in $\%)$	14.720	12.440	Bureau of Labor Statistics (BLS)
Matching eff. shock persistence* ρ_{ME}	0.977	0.977	Sedláček (2014)
Matching eff. shock volatility* σ_{ME}	0.040	0.040	Sedláček (2014)

Notes: This table reports the calibration targets and the model moments. Model moments are computed from the ergodic distribution of the global solution. Data sources: BLS (LNS13000000, LNS14000000) and Barnichon (2010).

5.3 Beveridge curve in Equilibrium: validating the paradox

We now examine the global nonlinear solution to determine if the "churning channel" identified in Theorem 1 is quantitatively sufficient to generate the observed Beveridge curve dynamics. Figure 5 displays the equilibrium relationship between unemploy-

ment and vacancies for the baseline model (Panel a) and the exogenous separation counterfactual (Panel b), where points are color-coded by the state of matching efficiency.

Figure 5: Beveridge curve dynamics: Endogenous vs. Exogenous Separation

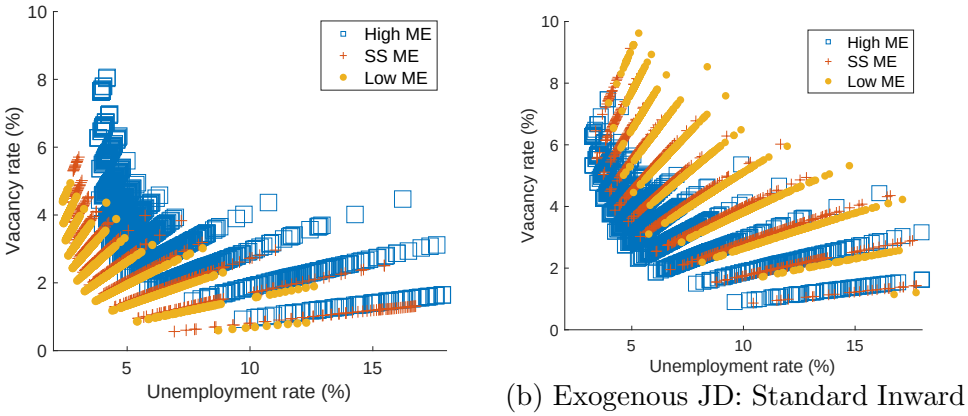

(a) Baseline: Paradoxical Outward Shift Shift

(b) Exogenous JD: Standard Inward

Notes: The figure plots the joint distribution of unemployment and vacancies from the global solution. Blue squares denote periods of high matching efficiency (+1 s.d.), while yellow crosses denote low efficiency (−1 s.d.).

The contrast between the two models confirms our theoretical predictions regarding the "efficiency paradox." In the baseline model with endogenous separations (Panel a), periods of high matching efficiency (indicated by blue squares) are associated with a distinct *outward* shift of the curve. Despite the ease of hiring, the equilibrium settles at higher unemployment and vacancy rates. This confirms that the elasticity condition in Theorem 1 holds in our calibration: the surge in endogenous separations outweighs the direct efficiency gain. In sharp contrast, the counterfactual model with exogenous separations (Panel b) shows that high matching efficiency always shifts the curve *inward*. Without the endogenous separation margin, easier hiring unambiguously lowers unemployment for any given vacancy level, failing to replicate the non-monotonic dynamics observed in the post-COVID data.

Notably, the baseline model with endogenous separations delivers a well-defined Beveridge-curve relationship, complementing earlier analyses such as Fujita and Ramey (2012). Our results suggest that Beveridge-curve implications in endogenous-separation environments can be quantitatively sensitive to calibration and to the accuracy of the nonlinear solution. By solving the model globally, we accurately capture reservation-productivity dynamics and cutoff-driven separations, yielding a coherent negative unemployment–vacancy relationship that shifts with matching efficiency.

To precisely quantify this non-linearity, Figure 6 plots the conditional average Beveridge curve across matching-efficiency bins, indexed from 1 (lowest) to 9 (highest). The contrast between panels crystallizes the paper's central result.[4] In the baseline model with endogenous separations (Panel a), the numbered points reveal a subtle but theoretically significant pattern. At low matching efficiency (points 1-5), the curve shifts weakly inward as efficiency rises—consistent with the standard intuition when the separation elasticity remains below the survival rate. The economy clusters in a tight region with unemployment around 4-4.5% and vacancies near 2.5-3%, with modest improvements in matching efficiency yielding modest gains. However, once efficiency crosses a threshold (points 6-9), the relationship reverses: each incremental improvement in matching efficiency now shifts the curve *outward*, with unemployment rising from 4.5% to over 7% and vacancies from 3% to nearly 6%. This is the quantitative signature of Theorem 1—the same model generates inward shifts at low efficiency and outward shifts at high efficiency, depending on whether the separation elasticity exceeds the survival rate.

Panel (b) provides the counterfactual. With exogenous separations, the numbered points trace a conventional downward-sloping Beveridge curve that shifts monoton-

[4]For Figure 6, we partition simulated realizations of m_t into 9 bins and plot conditional averages of the Beveridge curve across these bins. For solving the model and for the remaining quantitative exercises, we discretize the matching-efficiency process into 3 Tauchen nodes.

Figure 6: Nonlinear shifts of the Beveridge curve: conditional averages

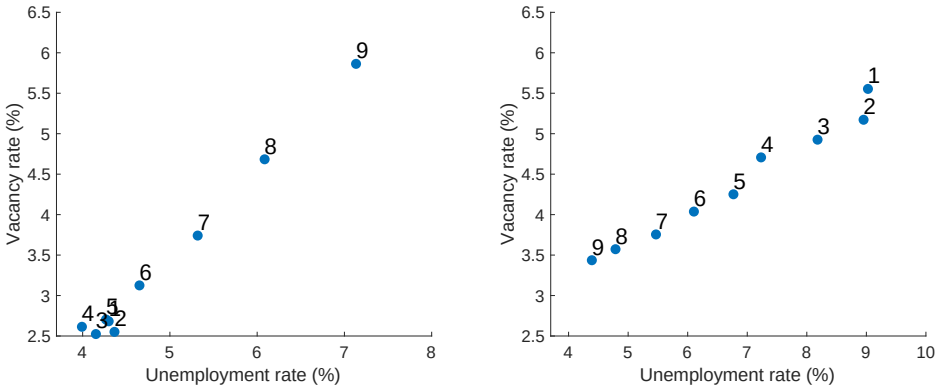

(a) Baseline (b) Exogenous JD

Notes: Each point represents the conditional average of unemployment and vacancies for a given matching efficiency state, indexed 1 (lowest) to 9 (highest). Panel (a): with endogenous separations, the curve shifts weakly inward at low efficiency (points 1–5) but sharply outward at high efficiency (points 6–9). Panel (b): with exogenous separations, the curve shifts monotonically inward across all efficiency levels.

ically inward as efficiency rises. Point 1 (lowest efficiency) sits at approximately 9% unemployment and 5.5% vacancies; point 9 (highest efficiency) reaches 4.5% unemployment and 3.5% vacancies. The inward shift is uniform across all efficiency levels—there is no regime change. The comparison highlights a key empirical implication: only the endogenous separation model can rationalize *both* the weak inward shifts observed during normal times *and* the sharp outward shifts during high-efficiency episodes like the post-COVID recovery. The exogenous separation model, by construction, predicts uniformly inward shifts regardless of the efficiency level.

The static outward shift has profound dynamic consequences for the economy's stability. Because high matching efficiency raises the reservation productivity threshold z_s, it leaves the economy with a fragile distribution of matches that are highly sensitive to negative shocks. Figure 7 illustrates this by plotting the generalized impulse response (GIRF) of unemployment to a negative TFP shock across different states. When the shock hits during a high-efficiency period (Panel a), the unem-

ployment response is significantly amplified. The initial mass of marginal workers is high due to the elevated reservation threshold, leading to a sharp wave of separations when productivity falls. Conversely, when efficiency is low (Panel b), the economy exhibits "labor hoarding" behavior; firms are already reluctant to separate due to high replacement costs, rendering the unemployment response more resilient to the shock. This state-dependence explains why recessions occurring during fluid labor market conditions can exhibit sharper unemployment spikes than those during stagnant periods.

Figure 7: State-dependent unemployment responses to a negative TFP shock

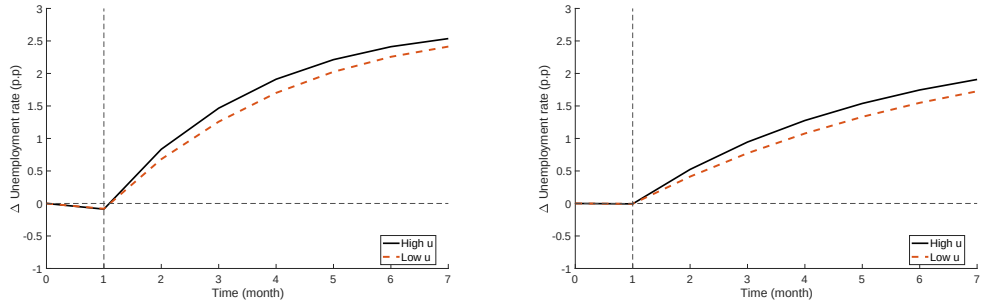

(a) Response during high ME (Fragile) (b) Response during low ME (Resilient)

Notes: Generalized impulse response functions of unemployment to a one-standard-deviation negative TFP shock, conditional on initial matching efficiency. "High u" and "Low u" denote high and low initial unemployment states, respectively. Panel (a): high matching efficiency amplifies the response via elevated endogenous separations. Panel (b): low matching efficiency induces labor hoarding, muting the response.

Finally, we assess the model's ability to reproduce historical volatility patterns. Figure 8 compares the model-implied unemployment series against U.S. data (dashed red line). The baseline model (Panel a) successfully captures the large spikes in unemployment volatility observed in the data, particularly during the high-efficiency episodes shaded in blue. In contrast, the exogenous separation model (Panel b) predicts a counterfactually smooth unemployment path. By shutting down the churning channel, the exogenous model misses the explosive nature of unemployment during

reorganization episodes. This confirms that endogenous separations are not merely a theoretical mechanism but a quantitative necessity for tracking the volatility of U.S. labor market dynamics.

Figure 8: Model fit: matching historical volatility

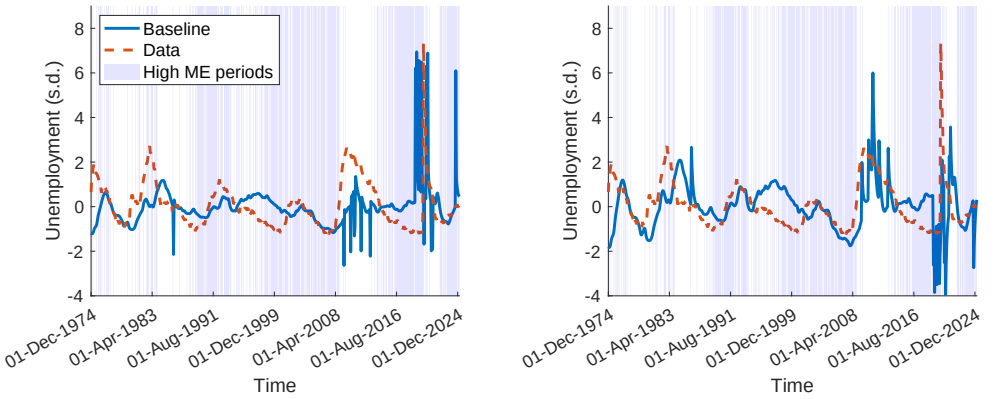

(a) Baseline (Endogenous Sep) (b) Counterfactual (Exogenous Sep)

Notes: Model-implied unemployment (solid blue) versus U.S. data (dashed red), expressed in standard deviations from mean. Shaded regions denote high matching efficiency periods (+1 s.d. above trend). Sample period: 1974–2024. The baseline model captures unemployment spikes during high-ME episodes; the exogenous separation model generates counterfactually smooth dynamics.

6 Efficiency and policy analysis

Theorem 1 shows that high matching efficiency can raise endogenous separations through the churning channel, generating outward Beveridge-curve shifts. This section asks whether the resulting volatility is efficient, and if not, what simple instruments can mitigate it.

6.1 A constrained-efficient benchmark: the Hosios path

In canonical search models, the decentralized equilibrium is constrained efficient when the surplus-sharing rule internalizes the matching congestion externality (Hosios,

1990). Formally, efficiency requires the worker's bargaining weight to equal the unemployment elasticity of the matching function:

$$\eta_t^* = \frac{\partial M(U_t, V_t)}{\partial U_t} \frac{U_t}{M(U_t, V_t)}. \tag{39}$$

Under a CES matching function, this elasticity varies with tightness, making η_t^* time-varying. The baseline economy instead features a fixed Nash weight η, so the Hosios condition holds only at the calibrated steady state and generally fails along the transition path.

We compute a *Hosios-efficient global path* by solving the same economy under identical aggregate shocks, but allowing the bargaining weight to adjust endogenously each period as $\eta_t = \eta_t^*(\theta_t)$. This benchmark corresponds to the allocation implemented by competitive search (Moen, 1997; Wright et al., 2021) and isolates the inefficiency induced by rigid surplus sharing in the presence of state-dependent tightness and endogenous separations.[5]

Figure 9 compares unemployment dynamics under the baseline (dotted) and Hosios-efficient (solid) economies. Panel (a) plots the time series under identical shock sequences. Two features stand out. First, unconditional mean unemployment is similar across both economies ($\approx 4.5\%$), indicating that the inefficiency is not primarily about levels. Second, the baseline economy exhibits markedly higher volatility: the standard deviation of unemployment is 10.58% versus 8.71% in the efficient benchmark—a 21% reduction in volatility from correcting the bargaining distortion.

Panel (b) reveals the source of this excess volatility. The scatter plot shows the deviation of baseline unemployment from the Hosios benchmark ($u_t - u_t^{\text{Hosios}}$) against

[5]Our use of the Hosios path is benchmark-based rather than welfare-optimal: we do not solve for an optimal policy under a welfare criterion. Instead, we compute the Hosios-efficient allocation as a constrained-efficient reference and then ask what simple wedge on vacancy creation would *implement* (i.e., replicate) that allocation in the decentralized economy

the level of baseline unemployment. The relationship is steeply positive: when unemployment is low (around 4–5%), the baseline tracks the efficient path closely. But as unemployment rises, the gap widens dramatically—reaching 4 percentage points when baseline unemployment exceeds 15%. This pattern confirms that the inefficiency concentrates in high-unemployment states, precisely when the churning channel is most active.

The mechanism is as follows. During high-efficiency episodes, the fixed bargaining weight prevents wages from rising sufficiently to temper vacancy creation. Firms, facing low expected hiring costs, raise the reservation productivity threshold z_s aggressively. The efficient planner, by contrast, would raise the bargaining weight η_t^* as tightness increases, transferring more surplus to workers and moderating vacancy posting. This chokes off the excessive churn that characterizes the decentralized equilibrium.

Figure 9: The Efficiency Gap: Baseline vs. Hosios-Efficient Unemployment

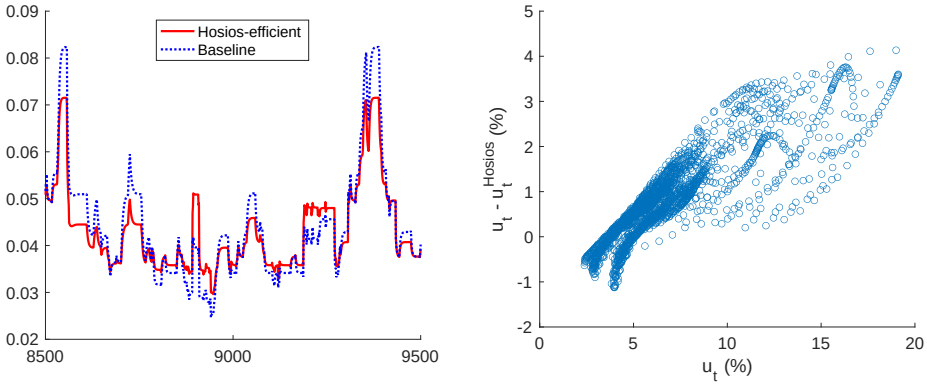

(a) Unemployment Time Series (b) Deviation from Efficiency

Notes: Panel (a): unemployment under the baseline economy with fixed bargaining weight (dotted) and the Hosios-efficient economy with state-contingent η_t^* (solid), simulated under identical shock sequences. Panel (b): deviation of baseline unemployment from Hosios benchmark versus baseline unemployment level. The positive slope indicates that inefficiency concentrates in high-unemployment states.

Table 7 quantifies the state-dependence of these deviations. In the baseline model,

the average absolute gap from Hosios is 0.44 percentage points during high-ME periods versus 0.34 during low-ME periods—a difference of 0.10 percentage points, or roughly 30% larger. For the exogenous separation model, this pattern reverses: the gap is *smaller* during high-ME periods (0.65 vs. 0.74), with a negative differential of −0.09.

In the exogenous separation model, high matching efficiency unambiguously improves outcomes, so the fixed bargaining weight distortion is less costly when efficiency is high. In the baseline model with endogenous separations, high matching efficiency triggers the churning channel, amplifying the cost of the bargaining distortion. The 0.19 percentage point swing in the differential (0.10 versus −0.09) is dominantly attributable to endogenous separations. This is further evidence that the churning channel is the primary source of inefficient volatility.

Table 7: Matching efficiency and the Hosios gap

	Average absolute distance from Hosios (%)			
	Baseline		Exogenous sep.	
	Unemp.	Vacancy	Unemp.	Vacancy
High ME	0.44	0.32	0.65	0.27
Low ME	0.34	0.21	0.74	0.42
Diff. $(High - Low)$	0.10	0.11	-0.09	-0.15

Notes: Average absolute deviation of unemployment and vacancies from the Hosios-efficient benchmark, by matching efficiency regime. "High ME" denotes periods with matching efficiency above median; "Low ME" below median. "Diff." is the difference in gaps between regimes. Positive differentials indicate inefficiency concentrates in high-ME periods.

6.2 Taming the churn: optimal corporate tax

The Hosios analysis in Section 6.1 establishes that the baseline economy generates excess unemployment volatility, concentrated in high-matching-efficiency states. We now ask whether a simple fiscal instrument can close this gap. We focus on a corporate tax τ levied on match output, which is equivalent to a firing penalty in this environment: by reducing the net value of a marginal match, the tax raises the cost of separation relative to retention, dampening the churning channel identified in Theorem 1.[6]

To evaluate this instrument in a historically relevant context, we compare the two most recent U.S. recessions—COVID-19 and the Great Recession—which exemplify opposite matching-efficiency regimes. We adopt the generalized impulse response function (GIRF) methodology based on the recursive competitive equilibrium developed in Lee (2025). For each recession, we identify a period along the model's global equilibrium path whose unemployment rate and matching efficiency most closely match pre-crisis conditions. The pre-COVID economy is characterized by low unemployment and high matching efficiency, placing it squarely in the regime where the churning channel is active. The pre–Great Recession economy, by contrast, features moderate unemployment and low matching efficiency—a regime where endogenous separations are muted and labor hoarding prevails. Starting from each identified state, we draw 1,000 independent shock sequences from the model's stochastic process, all sharing the same initial exogenous innovation, and average the resulting transition paths to construct the GIRF.

Figure 10 displays the results. Three paths are plotted for each recession: the

[6]Formally, the tax modifies the job destruction condition by replacing Az with $(1-\tau)Az$, compressing the firm's surplus and lowering the reservation threshold z_s for any given level of matching efficiency.

baseline response (solid line with markers), the Hosios-efficient response (solid line), and the response under the optimally chosen corporate tax (dashed line). The optimal tax rate is selected to minimize the L^2 distance between the policy-induced unemployment path and the Hosios-efficient path over the impulse response horizon.

Figure 10: State-dependent policy effectiveness

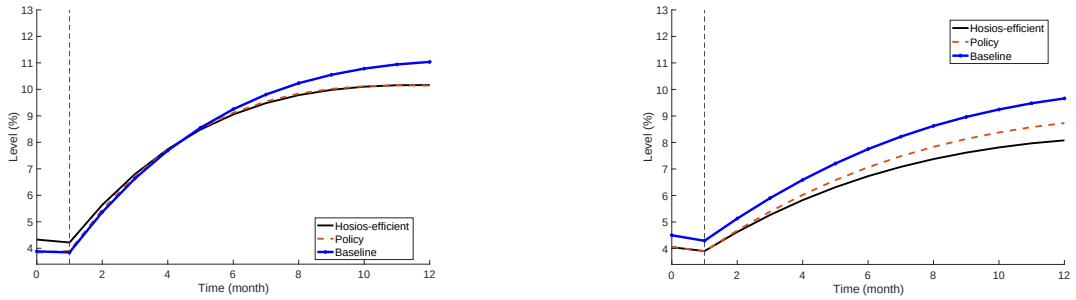

(a) COVID-19 recession (high m) (b) Great Recession (low m)

Notes: Generalized impulse response functions of unemployment for two recession episodes, constructed by averaging over 1,000 shock sequences from identical initial conditions. Solid line: Hosios-efficient path with state-contingent η_t^*. Solid line with markers: baseline with fixed η. Dashed line: baseline with optimal corporate tax ($\tau \approx 5\%$). Panel (a): pre-COVID initial conditions (low unemployment, high matching efficiency). Panel (b): pre–Great Recession initial conditions (moderate unemployment, low matching efficiency). The optimal tax is chosen to minimize the L^2 distance to the Hosios path.

During the COVID-19 recession (Panel a), the baseline economy generates an unemployment surge that substantially overshoots the efficient benchmark. This excess response reflects the mechanism identified in our theoretical analysis: high matching efficiency lowers expected hiring costs, causing firms to raise the reservation threshold z_s aggressively and shed marginal matches. The Hosios-efficient planner avoids this by raising the bargaining weight η_t^* as tightness increases, transferring surplus to workers and moderating vacancy creation. The optimal corporate tax replicates this outcome through a different channel: by compressing match surplus directly, a tax of approximately 5% reduces the sensitivity of z_s to matching efficiency fluctuations, effectively acting as a circuit breaker on the separation elasticity $\partial \log s / \partial \log m$. The

dashed line tracks the Hosios path closely, confirming that this simple instrument can approximate the constrained-efficient allocation during high-efficiency episodes.

The Great Recession (Panel b) provides a revealing contrast. With matching efficiency low, the churning channel is largely dormant: the reservation threshold sits in the low-density tail of the productivity distribution, and endogenous separations contribute little to unemployment dynamics. Consequently, the baseline and Hosios-efficient paths are much closer to each other, and the optimal tax has a correspondingly smaller effect. This state-dependence is consistent with the pattern documented in Table 7: the Hosios gap widens during high-ME periods and narrows during low-ME periods.

The policy implication is that the welfare case for firing costs is state-dependent. In fluid labor markets where matching efficiency is elevated, moderate firing costs can yield substantial welfare gains by dampening inefficient churn without materially affecting mean unemployment. In slack labor markets, the same instrument is largely redundant. This suggests that well-designed stabilization policy should be counter-cyclical not merely in the level of intervention but in the *type* of instrument deployed: firing penalties are most valuable precisely when labor markets appear healthiest.

The preceding analysis shows that a well-targeted instrument can approximate the efficient allocation. We now demonstrate that policies designed without regard to the endogenous separation margin can substantially worsen outcomes.

6.3 Risks of ignoring endogenous separations

Finally, we use our framework to evaluate a standard stabilization policy in the form of counter-cyclical unemployment benefits. We consider a simple rule in which benefits b increase by 5% whenever unemployment exceeds 6.5%, capturing the spirit of

extended-benefit triggers used in U.S. policy.

Table 8 compares the effects of this rule in our baseline economy and in the exogenous-separation counterfactual. The results reveal a stark difference in policy transmission.

Consider first mean unemployment. In both models, counter-cyclical benefits raise average unemployment—an expected consequence of increasing the worker's outside option and reducing match surplus. The magnitudes are similar: +0.64 percentage points in the baseline (from 4.59% to 5.23%) and +0.66 percentage points with exogenous separations (from 6.84% to 7.51%). On this margin, the models deliver comparable predictions.[7]

Table 8: The Impact of Counter-Cyclical Unemployment Benefits

	Unconditional		High ME		Low ME	
	$\mathbb{E}(u_t)$	$\sigma(u_t)$	$\mathbb{E}(u_t)$	$\sigma(u_t)$	$\mathbb{E}(u_t)$	$\sigma(u_t)$
baseline	4.591	10.829	5.566	11.904	4.066	13.936
baseline + counter-cyclical b	5.229	15.167	6.610	18.903	4.378	17.957
exo. sep.	6.843	11.343	5.624	13.470	8.129	13.844
exo. sep. + counter-cyclical b	7.507	13.866	6.090	17.161	8.983	16.900

Notes: The table reports mean unemployment $\mathbb{E}(u_t)$ and unemployment volatility $\sigma(u_t)$ under the baseline policy (b fixed) and counter-cyclical policy (b increases by 5% when $u_t > 6.5\%$). "High ME" and "Low ME" denote periods with matching efficiency above and below median, respectively. Volatility is expressed as coefficient of variation (%). The baseline model features endogenous separations; the exogenous separation model fixes the separation rate at its steady-state value.

The divergence emerges in volatility. In the exogenous-separation model, the policy raises unemployment volatility by 22% (from 11.34% to 13.87%). In the base-

[7]The two economies differ in their baseline mean unemployment because the exogenous-separation counterfactual is disciplined by a different set of moments; our volatility results are robust to recalibrating the counterfactual to match mean unemployment.

line model with endogenous separations, the same policy raises volatility by 40% (from 10.83% to 15.17%). The amplification is even stronger during high-matching-efficiency periods: volatility increases by 59% in the baseline (from 11.90% to 18.90%) compared to 27% in the exogenous-separation model.

The mechanism operates through the reservation-productivity threshold. Higher unemployment benefits raise the worker's outside option, compressing the firm's surplus from a marginal match. Firms respond by raising the reservation threshold z_s, endogenously increasing separations among low-productivity matches. In the exogenous-separation model, this channel is shut down: the separation rate is fixed, so benefits affect only the job-creation margin. In the baseline model, the separation margin creates an amplification loop: higher benefits $\rightarrow$ higher z_s $\rightarrow$ more separations $\rightarrow$ higher unemployment, which increases the time spent in the high-benefit regime and further tightens the threshold.

State dependence reinforces this concern. During high-matching-efficiency periods, the reservation threshold is already elevated due to the churning channel. Counter-cyclical benefits therefore push z_s into a higher-density region of the match-productivity distribution, triggering disproportionately large separation responses. As a result, policy evaluations based on exogenous-separation models can substantially understate the volatility consequences of benefit expansions in high-efficiency states.

More broadly, policies that raise the worker's outside option or reduce match surplus can interact with endogenous separations in similar ways. Our framework provides a quantitative tool to assess these amplification effects in a nonlinear environment.

7 Concluding remarks

This paper develops a globally solved Diamond-Mortensen-Pissarides model with endogenous job destruction to study nonlinear Beveridge curve dynamics. We establish a sharp theoretical result: the Beveridge curve shifts outward when matching efficiency rises if and only if the elasticity of job separation with respect to matching efficiency exceeds the match survival rate. This condition overturns the standard intuition that improvements in matching technology unambiguously reduce the level of unemployment, given the level of vacancies. Moreover, it provides a unified explanation of the divergent dynamics observed during the Great Financial Crisis and Recession and during the COVID-19 shutdown and recovery.

Two broader implications emerge from our globally solved model. First, efficiency and stability are not complements in the labor market. The same forces that make labor markets fluid—low hiring costs, rapid reallocation—also make them fragile. Policymakers face a genuine trade-off: improving matching efficiency may simultaneously amplify unemployment volatility and increase the cyclicality of employment. This trade-off is absent from exogenous-separation models that dominate quantitative policy analysis.

Second, the welfare costs of labor market fluctuations may be higher than previously recognized. When separations are endogenous, high-efficiency states generate inefficient volatility—churn that imposes real costs without serving allocative purposes. Our finding that a modest corporate tax reduces unemployment volatility substantially without raising mean unemployment suggests stabilization policy deserves renewed attention.

These results suggest a broader agenda for macro-labor research: moving beyond the study of frictional unemployment *levels* to understanding the welfare consequences

of *turnover volatility* itself. Future work should explore how this endogenous instability interacts with inflation dynamics and the design of social insurance in markets characterized by rapid reallocation.

References

Barlevy, Gadi, R Jason Faberman, Bart Hobijn, and Ayşegül Şahin. 2024. "The Shifting Reasons for Beveridge Curve Shifts." *Journal of Economic Perspectives* 38 (2):83–106.

Barnichon, Regis. 2010. "Building a composite help-wanted index." *Economics Letters* 109 (3):175–178.

Barnichon, Régis and Adam Hale Shapiro. 2024. "Phillips Meets Beveridge." *Journal of Monetary Economics* :103660.

Crump, Richard K., Stefano Eusepi, Marc Giannoni, and Ayşegül Şahin. 2024. "The unemployment–inflation trade-off revisited: The Phillips curve in COVID times." *Journal of Monetary Economics* 145:103580. URL https://www.sciencedirect.com/science/article/pii/S0304393224000333. Inflation: Expectations & Dynamics October 14-15, 2022.

Den Haan, Wouter J, Garey Ramey, and Joel Watson. 2000. "Job destruction and propagation of shocks." *American Economic Review* 90 (3):482–498.

Elsby, Michael WL, Bart Hobijn, and Ayşegül Şahin. 2015. "On the importance of the participation margin for labor market fluctuations." *Journal of Monetary Economics* 72:64–82.

Fujita, Shigeru and Garey Ramey. 2012. "Exogenous versus endogenous separation." *American Economic Journal: Macroeconomics* 4 (4):68–93.

Hagedorn, Marcus and Iourii Manovskii. 2008. "The cyclical behavior of equilibrium unemployment and vacancies revisited." *American Economic Review* 98 (4):1692–1706.

Hodrick, Robert J and Edward C Prescott. 1997. "Postwar US business cycles: an empirical investigation." *Journal of Money, credit, and Banking* :1–16.

Hosios, Arthur J. 1990. "On the efficiency of matching and related models of search and unemployment." *The Review of Economic Studies* 57 (2):279–298.

Jung, Philip and Keith Kuester. 2015. "Optimal labor-market policy in recessions." *American Economic Journal: Macroeconomics* 7 (2):124–156.

Lee, Hanbaek. 2025. "Global Nonlinear Solutions in Sequence Space and the Generalized Transition Function." *Working paper* .

Moen, Espen R. 1997. "Competitive search equilibrium." *Journal of political Economy* 105 (2):385–411.

Mortensen, Dale T and Christopher A Pissarides. 1994. "Job creation and job destruction in the theory of unemployment." *The Review of Economic Studies* 61 (3):397–415.

Petrongolo, Barbara and Christopher A. Pissarides. 2001. "Looking into the Black Box: A Survey of the Matching Function." *Journal of Economic Literature* 39 (2):390–431.

Petrosky-Nadeau, Nicolas and Lu Zhang. 2017. "Solving the Diamond–Mortensen–Pissarides model accurately." *Quantitative Economics* 8 (2):611–650.

———. 2021. "Unemployment crises." *Journal of Monetary Economics* 117:335–353. URL https://www.sciencedirect.com/science/article/pii/S0304393220300064.

Pissarides, Christopher A. 2000. *Equilibrium unemployment theory*. MIT press.

Rotemberg, Julio J. 1999. "A heuristic method for extracting smooth trends from economic time series."

Sedláček, Petr. 2014. "Match efficiency and firms' hiring standards." *Journal of Monetary Economics* 62:123–133.

Shimer, Robert. 2005. "The cyclical behavior of equilibrium unemployment and vacancies." *American Economic Review* 95 (1):25–49.

Wright, Randall, Philipp Kircher, Benoît Julien, and Veronica Guerrieri. 2021. "Directed search and competitive search equilibrium: A guided tour." *Journal of Economic Literature* 59 (1):90–148.

Yashiv, Eran. 2007. "Labor search and matching in macroeconomics." *European Economic Review* 51 (8):1859–1895.